doi:10.22306/am.v5i4.69

Received: 19 Oct. 2020
Revised: 21 Nov. 2020
Accepted: 14 Dec. 2020

DESIGN AND FABRICATION OF RUNNING CHEETAH MECHANICAL TOY USING FOUR-BAR LINKAGE

Adimas Wicaksana
Universitas Pamulang, Jl. Surya Kencana no. 1 Pamulang, dosen01678@unpam.ac.id

Keywords: four-bar linkage, mechanism design, 3D printing

Abstract: Four-bar is the simplest planar 1-DOF closed loop linkage. It has been studied for centuries for its versatility and simplicity. In this paper a novel design method to obtain a four-bar linkage given a path and its endpoints will be presented. This method will then be applied to a case study of making a model that produces a specified movement based on reference animation. The mechanism obtained had an average root-mean-square of position error of roughly 14.3 pixels for front leg and 25.9 pixels for hind leg. This number is quite small compared to the perimeter of the traced path, which are 530 pixels and 617 pixels for front leg and hind leg respectively. A prototype model of the designed mechanism was fabricated to verify its manufacturing viability and to confirm the correctness of the path generated.

1 Introduction

There has been quite a considerable interest in development of motion guided toy following the publication of a seminal work by Zhu et al [1]. Recent developments include T-Rex, Pushing Man and Dog toy [2], Bull toy and Dancing Lantern [3], and Dancing Automaton [4] from motion capture sequence. However, the commonality between the designs of all these toys is that they are machine elements that are relatively difficult to produce like gears and cams. These elements would require motion in at least two axes to be produced correctly. This would mean that one would require a CNC machine to produce the mechanism. One solution to simplify the mechanism would be to use one of the simplest planar mechanism, which is a four-bar linkage. Unfortunately, most of the case study for four-bar design has been focusing mostly on straight lines [5], circle [6], and figure-eight-like motions [7]. Most of the current work also seems to focus on Evolutionary Algorithm/Genetic Algorithm whose emphasis is on letting the computer attempt optimize four-bar parameter by itself without any additional heuristic from human [8,9] however the effectiveness of these techniques depends highly on initial position chosen. There is no guarantee that there will be convergence during solution space exploration. With recent advances in technology, it is already possible to do a brute force on four bar search space as long as correct assumptions are made [10,11]. However even using aforementioned software it still takes quite a long time to finish the search (roughly 4 hours). There are also works on synthesizing function [12,13] but those studies are orthogonal to ours as their works focuses on making a connection between input angle and output angle while our works focuses on creating motion based on prescribed path. This work attempts to bridge the existing hole in the study by providing an algorithm that can produce four bar that is capable of producing the desired walking motion within more reasonable time limit.

After the design is finalized a prototype was fabricated using combination of additive (3D Printing) and traditional subtractive manufacturing. This is to ensure both the viability of the mechanism (no interference) and the validity of the claim mentioned previously (that a CNC machine is not necessary to produce the desired motion). While we still require the use of 3D printer to produce the body of the toy its use is less pronounced compared to previous works. 3D Printing has enjoyed quite immense popularity in the recent year mainly due to major patents expiring sometime in 2009 [10]. It works by depositing molten plastic on top of moving base layer by layer. It has been used for research in various fields such as microfluidics [15,16], optics [17,18], biomedicine [19], and even aerospace [20].

2 Design

First consider a four-bar linkage that reaches a limiting point at position 1 and 3 as shown in figure 1. In this text notation similar to that of Sandor-Erdman [21] will be used

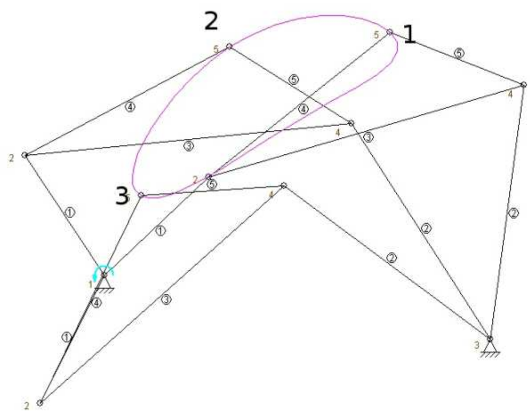

Figure 1 Four-bar Linkage with 2 Endpoints

A typical four-bar linkage design is typically done by splitting the linkages into two parts called dyads. Equations

Volume: 5 2020 Issue: 4 Pages: 53-60 ISSN 2453-7306

for both dyads can then be solved simultaneously. Let us initially consider the left dyad that contains the prime mover and ignore the right dyad as shown in figure 2.

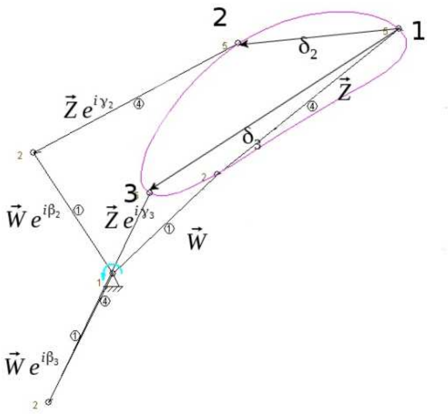

Figure 2 Left Dyad

From figure 2 we can see that the curves endpoints are reached when W and Z either points to the same direction or exact opposite of each other so we can get (1).

$$\vec{W} = a\vec{Z} \tag{1}$$

Where a is a scalar signifying the ratio of length of Z with respect to length of W.

Note that this is a sufficient but not necessary condition as there are cases where the endpoint is reached without W and Z pointing to the same direction or opposite to each other but as we can see in the case study later the search space for our method is wide enough that we won't need to consider all the possible cases (2).

$$\vec{\mathbf{W}}(\mathbf{e}^{\mathbf{i}\beta_3} - \mathbf{1}) + \vec{\mathbf{Z}}(\mathbf{e}^{\mathbf{i}\gamma_3} - \mathbf{1}) = \vec{\boldsymbol{\delta}}_3 \tag{2}$$

But we know that at position 3 W and Z points to opposite direction as compared to position 1 so we have (3).

$$\vec{W}e^{i\beta_3} = -a\vec{Z}e^{i\gamma_3} \tag{3}$$

Substituting Z from this equation (4) into (2)

$$\boldsymbol{W} = \frac{\vec{\boldsymbol{\delta}}_3}{\mathbf{e}^{\mathbf{i}\beta_3}(\mathbf{1}-\mathbf{a})-(\mathbf{1}+\mathbf{a})} \tag{4}$$

Similarly for position 2 we have (5)

$$\vec{\mathbf{W}}(\mathbf{e}^{\mathbf{i}\beta_2} - \mathbf{1}) + \vec{\mathbf{Z}}(\mathbf{e}^{\mathbf{i}\gamma_2} - \mathbf{1}) = \vec{\boldsymbol{\delta}}_2 \tag{5}$$

By substituting W and Z from (4) and (1) respectively we can get (6).

$$\frac{\vec{\boldsymbol{\delta}}_3}{\mathbf{e}^{\mathbf{i}\beta_3}(\mathbf{1}-\mathbf{a})-(\mathbf{1}+\mathbf{a})}(\mathbf{e}^{\mathbf{i}\beta_2} - \mathbf{1}) + \frac{\vec{\boldsymbol{\delta}}_3}{\mathbf{e}^{\mathbf{i}\beta_3}(\mathbf{1}-\mathbf{a})-(\mathbf{1}+\mathbf{a})}(\mathbf{e}^{\mathbf{i}\gamma_2} - \mathbf{1}) = \vec{\boldsymbol{\delta}}_2 \tag{6}$$

These are two equations (real and imaginary part) with 4 unknowns in β2, β3, γ2, and a. Since β2 and β3 are angles we can choose any number from 0 to 2π as our selections. Alternatively, if timings are important we can predetermine β2 and β3 since those angles correspond to crank angle for position 2 and 3. Either way for each pairs of β2, β3 we will have corresponding solutions in γ2 and a since each tuples must fulfil (6).

$$\begin{gathered}\mathbf{1} + \mathbf{2}\boldsymbol{a} + \boldsymbol{a}^{\mathbf{2}} - \cos(\beta_2) - \mathbf{a}\cos(\beta_2) - \cos(\beta_3) \\ +\boldsymbol{a}^{\mathbf{2}}\cos(\beta_3) + \cos(\beta_2)\cos(\beta_3) - \boldsymbol{a}\cos(\beta_2)\cos(\beta_3) \\ \mathbf{a}\cos(\gamma_2) - \mathbf{a}^{\mathbf{2}}\cos(\gamma_2) + \boldsymbol{a}\cos(\beta_3)\cos(\gamma_2) \\ -\mathbf{a}^{\mathbf{2}}\cos(\gamma_2)\cos(\beta_3) + \sin(\beta_2)\sin(\beta_3) - \\ \mathbf{a}\sin(\beta_2)\sin(\beta_3) + \boldsymbol{a}\sin(\boldsymbol{\beta}_3)\cos(\gamma_2) \\ -\boldsymbol{a}^{\mathbf{2}}\sin(\boldsymbol{\beta}_3)\cos(\gamma_2) \\ = \boldsymbol{Re}\left(\frac{\vec{\delta}_2}{\vec{\delta}_3}\right)(\mathbf{2}(\mathbf{1}+\boldsymbol{a}^{\mathbf{2}}) + (-\mathbf{1}+\boldsymbol{a}^{\mathbf{2}})\cos(\boldsymbol{\beta}_3))\end{gathered} \tag{7}$$

We can solve this equation (7) by replacing cos γ_2 with x and sin γ_2 with $\sqrt{(1-x^2)}$. By collecting all terms with x on one side and $\sqrt{(1-x^2)}$ on the other and squaring both sides we can get quadratic equation in x. We can then represent x in terms of a (8). Next, we take a look at the imaginary part of (6).

$$\begin{gathered}-\sin(\beta_2) - \mathbf{a}\ \sin(\beta_2) + \cos(\beta_3)\sin(\beta_2) \\ -\mathbf{a}\cos(\beta_3)\sin(\beta_2) + \sin(\beta_3) - \boldsymbol{a}^{\mathbf{2}}\sin(\beta_3) \\ -\cos(\beta_2)\sin(\beta_3) + \boldsymbol{a}\cos(\beta_2)\sin(\beta_3) \\ -\mathbf{a}\cos(\gamma_2)\sin(\beta_3) + \mathbf{a}^{\mathbf{2}}\cos(\gamma_2)\sin(\beta_3) \\ -\mathbf{a}\sin(\gamma_2) - \mathbf{a}^{\mathbf{2}}\sin(\gamma_2) + \mathbf{a}\cos(\beta_3)\sin(\gamma_2) \\ -\mathbf{a}^{\mathbf{2}}\cos(\beta_3)\sin(\gamma_2) \\ = \boldsymbol{Im}\left(\frac{\vec{\delta}_2}{\vec{\delta}_3}\right)(\mathbf{2}(\mathbf{1}+\boldsymbol{a}^{\mathbf{2}}) + (-\mathbf{1}+\boldsymbol{a}^{\mathbf{2}})\cos(\boldsymbol{\beta}_3))\end{gathered} \tag{8}$$

Since x is cos γ_2 and $\pm\sqrt{(1-x_2)}$ is sin γ_2 we can replace all terms that contains γ_2 with either of those terms. We can then substitute x value with representation found from (7). The resulting equation only contains one unknown which is a, which can then find by numerically solving for the polynomials. Note that not all a that is found is a valid solution since there is possibility that x >1, x<-1 or even x is imaginary. That is why we will need to double check the solutions found against (5).

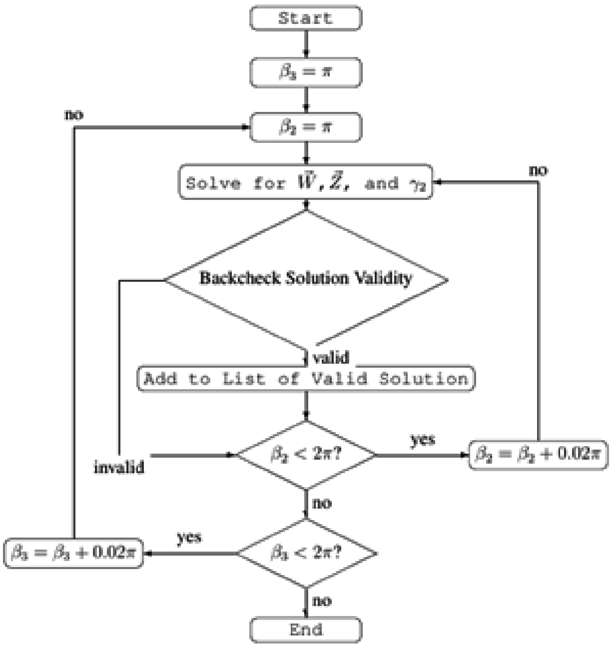

Figure 3 Left Dyad Design Procedure

Now let's take a look at the right dyad as depicted in figure 3.

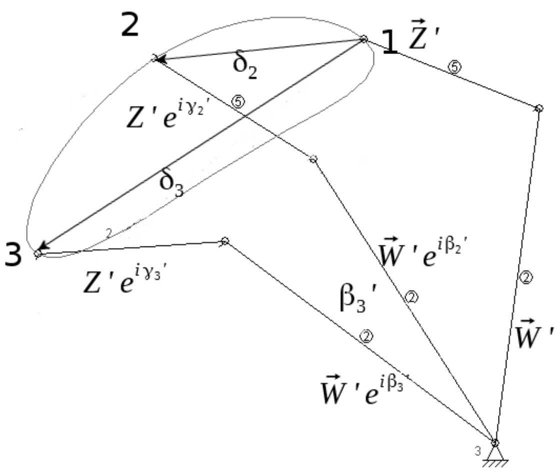

Figure 4 Right Dyad

Similarly the other dyad satisfy equation (2) and (5) as well (9).

$$\vec{\mathbf{W}}'\left(\mathbf{e}^{\mathbf{i}\beta_2'} - \mathbf{1}\right) + \vec{\mathbf{Z}}'(\mathbf{e}^{\mathbf{i}\gamma_2} - \mathbf{1}) = \vec{\boldsymbol{\delta}}_2 \qquad (9)$$

The prime symbol represents the counterpart for the right dyad. There is no prime symbol for $\gamma 2$ because the rotation angles are the same for both left and right dyad.

$$\vec{\mathbf{W}}'\left(\mathbf{e}^{\mathbf{i}\beta_3'} - \mathbf{1}\right) + \vec{\mathbf{Z}}'(\mathbf{e}^{\mathbf{i}\gamma_3} - \mathbf{1}) = \vec{\boldsymbol{\delta}}_3 \qquad (10)$$

So now we have four equations with 6 unknowns. Like the previous dyad we will iterate through both β2' and β3' from 0 to 2π. Likewise for each pairs we will generate its corresponding W' and Z'. Since (9) and (10) are linear equations in those two variables solving them should be pretty straightforward.

Once we have found the tuples (W, Z, W', Z') we have practically defined the four-bar linkage. We can then determine the suitability of the said linkage by considering the following:

1. Grashof Criterion.

Grashof criterion says that the sum of the longest link and the shortest link should be less than the sum of two remaining links. We can find the length of each links by taking the magnitude of vectors **W**, **W**, (**Z-Z'**), and (**W+Z-W'-Z'**) respectively.

2. Crank-rocker or Drag link configuration.

For a fourbar to make a complete rotation the shortest link needs to be either the ground or the input link. In other words among the four linkages either **W** or **W+Z-W'-Z'** needs to be the smallest of the four.

3. None of the coupler angles are imaginary.

We find every coupler angles for each input angle rotation that we are interested in using forward kinematics and verify that none of them are imaginary to make sure that we have a valid linkage.

4. Attempt to minimize the distance between each coupler positions and the supposed position.

We can do this by choosing angle combinations β_2, β_3, β_2', β_3' where the (11) reaches minimum.

$$\sum(\mathbf{P}_{\mathbf{x}_{\mathbf{design}}} - \mathbf{P}_{\mathbf{x}_{\mathbf{ideal}}})^2 + \sum(\mathbf{P}_{\mathbf{y}_{\mathbf{design}}} - \mathbf{P}_{\mathbf{y}_{\mathbf{ideal}}})^2 \qquad (11)$$

Volume: 5 2020 Issue: 4 Pages: 53-60 ISSN 2453-7306

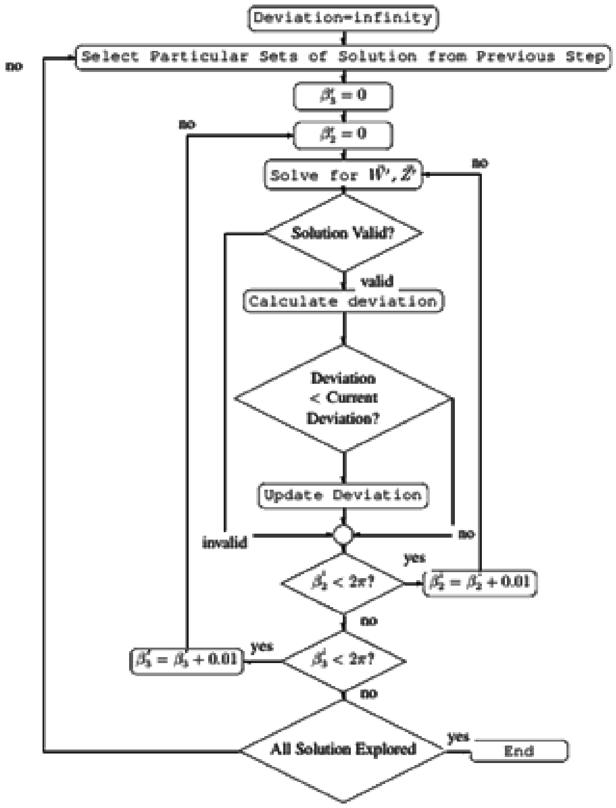

Figure 5 Right Dyad Design Procedure

3 Fabrication

First an animated image [22] was downloaded from the Internet to be used as a reference. For manufacturing simplicity, it is assumed that both left leg and right leg follows the same motion. The position of foreleg and hind leg at each frame is recorded in table 1. The leftmost and rightmost positions are selected as position 1 and 3 respectively. The positions where legs touch the ground is selected as position 2. We can then apply the calculation described in previous sections to the problem.

Ideally, we would like it so that each frame has similar spacing in β however attempting to pose this constraint tend to lead to unacceptable error in positions. As such the bottom part of the movement is time-stretched so that the error in positions can be minimized. Design for left dyad is implemented using Mathematica while the one for right dyad is implemented using Matlab. The linkage obtained is then simulated using software Artas SAM.

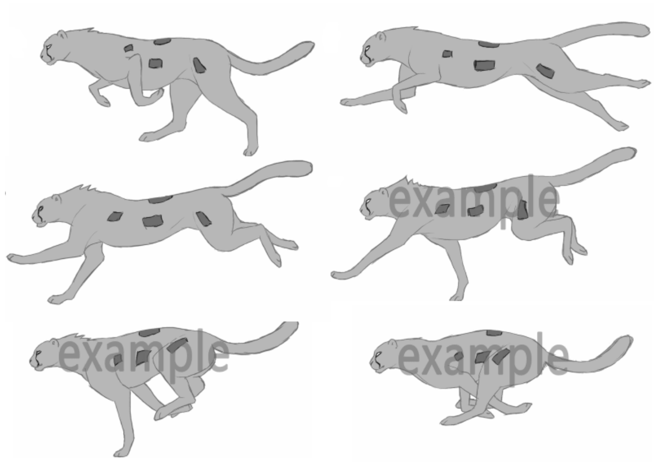

Figure 6 Reference Animation [22]

Table 1 Paw Positions in Pixel

Fore Leg (x)	**Fore Leg (y)**	**Hind Leg (x)**	**Hind Leg (y)**
0	32	125	44
8	31	165	12
63	0	297	3
149	3	343	24
215	56	381	43
231	68	391	91
197	66	377	90
187	79	341	58
143	63	340	62
96	60	294	48
51	63	244	48
11	69	197	50
13	66	149	62

After the design has been finalized each linkage was fabricated using combination of additive and subtractive manufacturing with conversion factor of 20 pixels/cm. Note that additive manufacturing process is not strictly required in the fabrication of the linkage. It is only used to shorten the waiting time while waiting for the raw material (acrylic) to arrive and to give good contrast whenever it is necessary. At the end of each linkage either a 3D-printed pin or a bearing was placed. For linkages made from acrylic the pin was connected by welding the pin into the acrylic using soldering iron. For linkages that are 3D-printed the pins are printed at the same time as the linkage. Bearings were placed by pushing them into the hole made either by drilling (for acrylic) or pre-made hole during printing (for 3D-printed part). The body of the toy was made by 3D-printing the part as well. Similarly, a bearing was also placed inside the body of the toy.

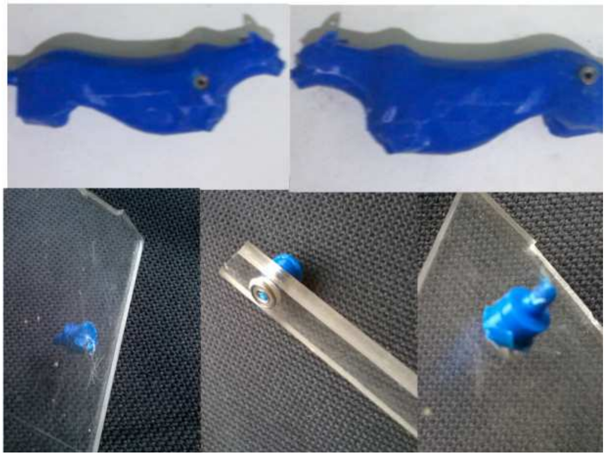

Figure 7 Revolute Joints

4 Results and Discussion

Figure 8 shows the linkage generated from our procedure that is to be connected to foreleg.

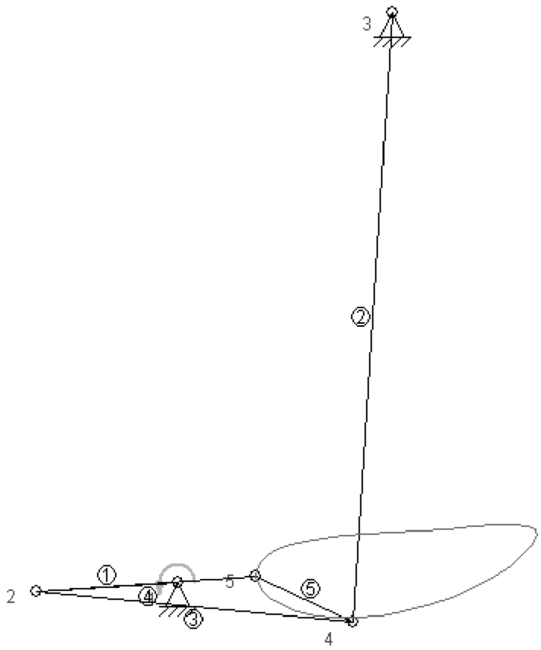

Figure 8 Front Leg Linkage

The crank has dimension of 5.8 cm, the rocker has dimension of 25 cm, the coupler has sides with dimensions of 4 cm, 9 cm, and 13 cm respectively. Meanwhile the frame (distance between pivots) is 25 cm long. We can still 3D-print the crank and the coupler while we need to use acrylic for the rocker since it is much larger than maximum size that Lulzbot can print. Meanwhile table 2 shows comparison between x and y generated by the linkage and the one from reference animation.

Table 2 Comparison between x and y positions of front leg

X Actual	X Reference	Y Actual	Y Reference
0.000	0.000	32.000	32.000
19.004	8.000	9.405	31.000
71.085	63.000	-2.191	0.000
142.769	149.000	8.352	3.000
206.101	215.000	38.736	56.000
230.999	231.000	68.000	68.000
217.926	197.000	74.837	66.000
183.068	187.000	73.392	79.000
135.030	143.000	69.378	63.000
87.450	96.000	66.336	60.000
48.860	51.000	62.653	63.000
21.311	11.000	55.885	69.000
4.908	13.000	45.348	66.000

As can be seen from table above the for the key frames (points 1, 2, and 3 during the design) are exact, meaning that the reference and actual positions as reached by the linkage are the same. By inserting these values into (11) we can get the squared-sum of position errors to be 2658 pixels, which corresponds to root-mean-square of 14.3 pixels, which are significantly smaller than the perimeter of the traced path (531 as measured by Autocad).

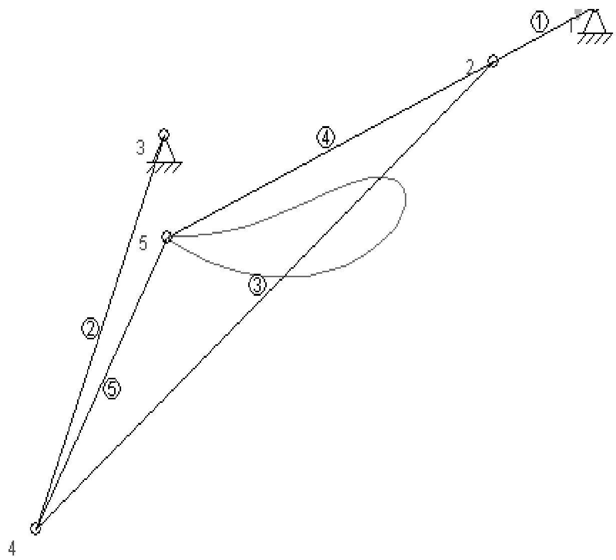

Figure 9 Hind Leg Linkage

The linkage for hind leg has crank with dimension of 6.3 cm, rocker with dimension of 20 cm, and coupler with sides of 34 cm, 20 cm, and 16 cm respectively. Distance between pivots is 25 cm long as well. Similarly, we can use 3D printer to produce the crank while the rocker and the coupler need to be made from acrylic.

Table 3 Comparison between x and y positions of hind leg

X Actual	X Reference	Y Actual	Y Reference
125.000	125.000	44.000	44.000
168.252	165.000	22.006	12.000
253.796	297.000	5.823	3.000
336.620	343.000	21.804	24.000
385.628	381.000	60.057	43.000
388.612	391.000	93.969	91.000
372.658	377.000	101.852	90.000
346.575	341.000	100.261	58.000
311.844	340.000	89.674	62.000
269.554	294.000	73.067	48.000
221.436	244.000	56.245	48.000
173.050	197.000	46.312	50.000
136.671	149.000	45.172	62.000

Similarly, for key frames the actual and reference positions are the same. Plugging these values into (11) will result in squared-sum of position error of 8718, which correspond to root-mean square of 25.9 pixels, which are much smaller than the perimeter of 616 as measured by Autocad.

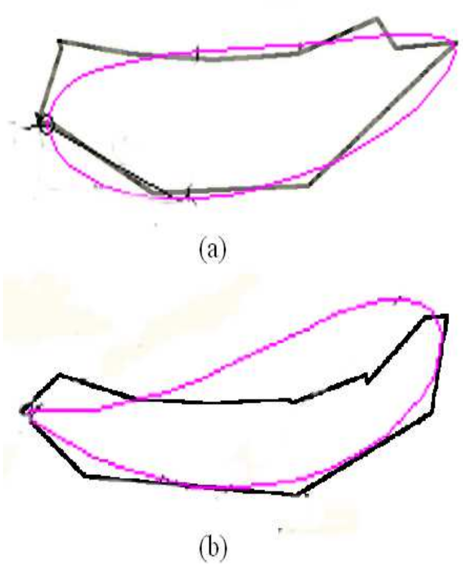

Figure 10 Visual Representation of Linkage Movement, Actual(pink) vs Reference(black), for front leg (a) and hind leg (b)

Figure 10 shows visual representation of these values so that we can evaluate the performance of the linkage qualitatively.

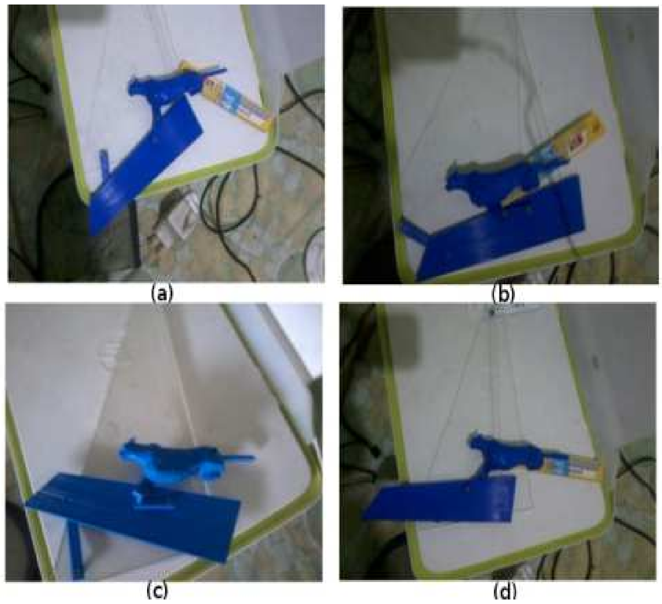

Figure 11 front leg mechanism at bottom-most (a), right-most (b), top-most(c), and left-most positions(d)

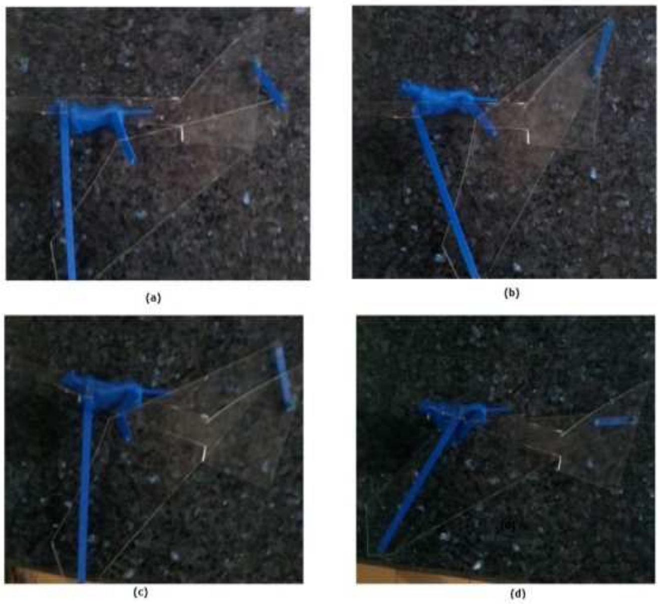

Figure 12 Fabricated mechanism at bottom-most (a), right-most (b), top-most(c), and left-most(d) positions

Prior to his work there have been several works that related to generating specific path for animation or motion capture purpose. Ceylan and Thomaszewski made some study regarding mechanism as internal part of the toy [3,4]. While their works are more elegant than ours it comes at a price of more complex assembly and manufacture. . In particular Ceylan's work requires the use of laser cutter and Thomaszewski's work requires 11 separate links compared to 5 links described in this paper. Our work is closer to the original work by Zu and Coros where the movers are completely separate from the toy [1,2]. While the problem is much simpler because it poses less constraints both of their work still requires more extensive manufacturing process where it requires either cam or gears inside the mechanism. In contrast four-bar linkage only uses a rigid link which is relatively simpler to manufacture because unlike gears or cam producing a rigid link only requires motion in single axis as compared to two or more for gears or cam.

5 Conclusion

Method to design four bar linkage based on its endpoints and a specified path has been presented. This method has been applied to generate a motion on a running cheetah toy. The designed mechanism was subsequently fabricated using traditional manufacturing method (no CNC) to demonstrate its manufacturing viability. Motion generated by the mechanism has relatively small error (less than 10x) compared to the total perimeter of the traced path. The linkage generated is also the simplest of all previous work. The procedure discussed in the text can also be applied to design pick-and-place mechanism where the workspace is constrained. Since the procedure actually take into account the limiting position of the coupler curve we can tell its endpoint quite easily.

References

[1] ZHU, L., XU, W., SNYDER, J., LIU, Y., WANG, G., GUO, B.: Motion-Guided Mechanical Toy Modeling, *ACM Transactions on Graphics*, Vol. 31, No. 6, pp. 1-10, 2012.

[2] COROS, S., THOMASZEWSKI, B., NORIS, G., SUEDA, S., FORBERG, M., SUMMER, R.W., MATUSIK, W., BICKEL, B.: Computational Design of Mechanical Characters, *ACM Transactions on Graphics*, Vol. 32, No. 4, pp. 1-12, 2013.

[3] THOMASZEWSKI, B., COROS, S., GAUGE, D., MEGARO, V., GRINSPUN, E., GROSS, M.: Computational Design of Linkage-Based Characters, *ACM Transactions on Graphics*, Vol. 33, No. 4, pp. 1-9, 2014.

[4] CEYLAN, D., LI, W., MITRA, N.J., AGRAWAKA, M., PAULY, M.: Designing and Fabricating Mechanical Automata from Mocap Sequences, *ACM Transactions on Graphics*, Vol. 32, No. 6, pp. 1-11, 2013.

[5] SLEESONGSOM, S., BUREERAT, S.: Four-Bar Linkage Path Generation through Self-Adaptive Population Size Teaching-Learning Based Optimization, *Knowledge-Based Systems*, Vol. 135, pp. 180-191, 2017.

[6] KIM, J.W., SEO, T., KIM, J.: A new design methodology for four-bar linkage mechanisms based on derivations of coupler curve, *Mechanism and Machine Theory*, Vol. 100, pp. 138-154, 2016.

[7] ZBIKOWSKI, R., GALINSKI, C., PEDERSEN, C.B.: Four-Bar Linkage Mechanism for Insect-like Flapping Wings in Hover: Concept and an Outline of Its Realization, *Journal of Mechanical Design*, Vol. 127, pp. 817-824, 2005.

[8] SINGH, R., CHAUDHARY, H., SINGH, A.K.: Defect-free optimal synthesis of crank-rocker linkage using nature-inspired optimization algorithms, *Mechanism and Machine Theory*, Vol. 116, pp. 105-122, 2017.

[9] ACHARYYA, S., MANDAL, M.: Performance of EAs for Four Bar Linkage Synthesis, *Mechanism and Machine Theory*, Vol. 44, pp. 1784-1794, 2009.

[10] HAUENSTEIN, J.D., SOTTILE, F.: Algorithm 921: AlphaCertified: Certifying Solutions to Polynomial Systems, *ACM Transansction on Mathematical Software*, Vol. 38, No. 4, pp. 1-20, 2012.

[11] WAMPLER, C., MORGAN, A., SOMMESE, A.: Complete solution of the Nine Point Path Synthesis Problem for Four-Bar-Linkages, *Transaction of the ASME*, Vol. 114, pp. 153–159, 1992

[12] LI, X., WEI, S., LIAO, Q., ZHANG, Y.: A Novel Analytical Method for Function Generation Synthesis of Planar Four-Bar Linkage, *Mechanism and Machine Theory 101*, Vol. 101, pp. 222–235, 2016

[13] FREUDENSTEIN, F.: Approximate Synthesis of Four-Bar Linkages, *Resonance*, Vol. 15, pp. 740-767, 2010.

[14] WAHEED, S., CABOT, J.M., MacDONALD, N.P., LEWIS, T., ROSANNE, M.G., PAULL, B., BREADMORE, M.C.: 3D printed microfluidic devices: enablers and barriers, *Lab on a Chip*, Vol. 16, pp. 1993-2013, 2016.

[15] HO, C.M.B., NG, S.H., LI, K.H.H.J., YOON, Y.: 3D printed microfluidics for biological applications, *Lab on Chip*, Vol. 15, No. 18, pp. 3627-3637, 2015.

[16] GONG, H., BICKHAM, B.P., WOOLLEY, A.T., NORDIN, G.P.: Custom 3D printer and resin for 18 μm × 20 μm microfluidic flow channels, *Lab on a Chip*, Vol. 17, No. 17, pp. 2899-2909, 2017.

[17] BUSCH, S.F., WEIDENBACH, M., FEY, M., SCHÄFER, F., PROBST, T., KOCH, M.: Optical Properties of 3D Printable Plastics in the THz Regime and their Application for 3D Printed THz Optics, *Journal of Infrared, Millimeter, and Terahertz Waves*, Vol. 35, No. 12, pp. 993-997, 2014.

[18] BUSCH, S.F., WEIDENBACH, M., BALZER, J.C., KOCH, M.: THz Optics 3D Printed with TOPAS, *Journal of Infrared, Millimeter, and Terahertz Waves*, Vol. 37, No. 4, pp. 303-307, 2016.

[19] INZANA, J.A., OLVERA, D., FULLER, S.M., KELLY, J.P., GRAEVE, O.A., SCHWARZ, E.M., KATES, S.L., AWAD, H.A.: 3D printing of composite calcium phosphate and collagen scaffolds for bone regeneration, *Biomaterials*, Vol. 35, No. 13, pp. 4026-4034, 2014.

[20] JOSHI, S.C., SHEIKH, A.A.: 3D printing in aerospace and its long-term sustainability, *Virtual*

and Physical Prototyping, Vol. 10, No. 4, pp. 175-185, 2015.

[21] SANDOR, G., ERDMAN, A.: *Advanced Mechanism Design: Analysis and Synthesis*, Vol. II, Englewood Cliffs, John Wiley and Sons, 1984.

[22] NORTHERNRED: Cheetah running cycle frames + PSD, [Online], Available: https://www.deviantart.com/northernred/art/Cheetah-running-cycle-frames-PSD-585490902 [20 Feb 2018], 2018.